*J. Fluid. Mech.* (1988), *vol.* 193, *pp.* 475–497
*Printed in Great Britain*



# Spiral structures and spectra in two-dimensional turbulence

By ANDREW D. GILBERT

Department of Applied Mathematics and Theoretical Physics, University of Cambridge, Silver Street, Cambridge CB3 9EW, UK

(Received 16 March 1987 and in revised form 26 November 1987)

Saffman argues that in decaying two-dimensional turbulence approximate discontinuities of vorticity will form, and the energy spectrum will fall off as $k^{-4}$. Saffman assumes that these discontinuities are well separated; in this paper, we examine how accumulation points of such discontinuities may give an energy spectrum of between $k^{-4}$ and $k^{-3}$. In particular we examine the energy spectra of spiral structures which form round the coherent vortices that are observed in numerical simulations of decaying two-dimensional turbulence. If the filaments of the spiral are assumed to be passively advected, the instantaneous energy spectrum has a $k^{-11/3}$ range. Thus we come some way to reconciling the argument of Saffman and the $k^{-3}$ energy spectrum predicted by models of quasi-equilibrium two-dimensional turbulence based on a cascade of enstrophy in Fourier space.

## 1. Introduction

Saffman (1971) argues that in decaying two-dimensional turbulence discontinuities in the vorticity field will form, since fluid elements with different values of (materially conserved) vorticity will be driven close together by the flow. These discontinuities will only be approximate, having a width $\delta$, which may be calculated by balancing diffusion and convection. Then the vorticity distribution along a line through the fluid will also possess approximate discontinuities, which Saffman assumes are separated by some average distance $L$. The Fourier transform of the vorticity distribution along such a line has a fall-off of $k^{-1}$, for $L^{-1} \ll k \ll \delta^{-1}$, and the energy spectrum may be calculated, giving $E(k) \propto k^{-4}$ in this range.

However, models of quasi-equilibrium two-dimensional turbulence which assume a local cascade of enstrophy in Fourier space (see, for example, Batchelor 1969; Kraichnan & Montgomery 1980) predict a $k^{-3}$ energy spectrum in an inertial range, which stretches from the scale of the forcing to the scale of viscous dissipation. Although these cascade models apply to quasi-equilibrium turbulence, whereas Saffman's argument is for decaying turbulence, there seems to be some conflict between the two predictions. Note that Saffman's argument relies on the material conservation of vorticity, which includes conservation of enstrophy, but also of other invariants, $\int \omega^n \, \mathrm{d}S$, $n = 3, 4, \ldots$. In this respect it is very different from the cascade models, which only conserve enstrophy and energy, discarding these further invariants.

Numerical simulations of two-dimensional turbulence (McWilliams 1984; Kida 1985; Brachet, Meneguzzi & Sulem 1986; Benzi, Patarnello & Santangelo 1987) suggest the following sequence of events in the process of decay. Initially vorticity gradients increase; separated sheets of high vorticity gradient form (Brachet *et al.*

1986; Kida 1985). Saffman's arguments apply, and the energy spectrum is observed to be approximately $k^{-4}$. However as time proceeds, these sheets accumulate (Brachet *et al.* 1986; Kida 1985) and the energy spectrum becomes shallower. At later times coherent vortices emerge in the flow (McWilliams 1984; Benzi *et al.* 1987) and most of the vorticity is concentrated in a small fraction of the fluid. These vortices move in the velocity field that they induce; occasionally two vortices will be driven sufficiently close that the stronger one will assimilate the weaker one by a winding-up process (McWilliams 1984; Melander, Zabusky & McWilliams 1987; Dritschel 1988). Coherent vortices are also seen in simulations of quasi-equilibrium two-dimensional turbulence (Herring & McWilliams 1985; Babiano *et al.* 1987; Legras, Santangelo & Benzi 1988).

Numerical simulations have yet to give a decisive determination of inertial-range spectral exponents in decaying and quasi-equilibrium two-dimensional turbulence. The difficulty is in obtaining the necessary separation between the scale of the forcing (quasi-equilibrium turbulence) or vortices (decaying turbulence), and the scale at which enstrophy dissipation occurs (Herring *et al.* 1974). In recent high-resolution simulations (Legras *et al.* 1988) of quasi-equilibrium two-dimensional turbulence an energy spectrum of about $k^{-3.5}$ has been observed at scales smaller than those of the coherent vortices. On the scales of the vortices, the spectrum shows a steep fall-off, which seems to arise from the statistical distribution of the sizes of vortices (Benzi *et al.* 1987). This may also account for the steep energy spectra observed by McWilliams (1984) in simulations of decaying flows with coherent vortices.

In this paper we shall be concerned with the later stages of the decay process, in which we may think of the vorticity as concentrated into coherent vortices. If we take the simplest model (figure 1*a*), in which the coherent vortices are without small-scale structure, then the vorticity distribution along a line possesses separated discontinuities. The energy spectrum falls off as $k^{-4}$, by Saffman's argument. If, however, we wish to account for the more complex interactions of vortices, indicated by numerical simulations, as well as possibly shallower spectra, we should incorporate more small-scale structure. H. K. Moffatt (personal communication) suggested that we should consider the vorticity as concentrated into coherent vortices with spiral structures (figure 1*b*), formed by the winding-up process. Now the distribution of vorticity along a line possesses accumulation points of discontinuities, on scales greater than $\delta$. This is more singular than a number of well-separated discontinuities, and leads to a slower fall-off than $k^{-1}$ in the Fourier transform of this distribution (Moffatt 1984). In §2, we consider a simple model, the wind-up of a weak vortex patch by a strong vortex core. We assume that the vortex patch is sufficiently weak that it may be treated as being passively advected by the vortex core. This model, although idealized, is intended to capture a clear physical effect, namely the winding-up of variations of vorticity by differential rotation and the accumulation of discontinuities. The energy spectrum of a single spiral structure (henceforth abbreviated to 'spiral') is calculated in §3, and has a range with a spectral power law of between $k^{-4}$ and $k^{-3}$. It is worth noting that a spectral power law in this range has been observed by Lesieur *et al.* (1988) in numerical simulations of the break-up of a mixing layer; this seems to be associated with the wind-up of vorticity variations about vortex cores.

The way in which spiral structures can modify the energy spectrum was discussed by Moffatt (1984) in the context of three-dimensional turbulence. This also appears to be a key to understanding Lundgren's (1982) 'strained spiral vortex model' of

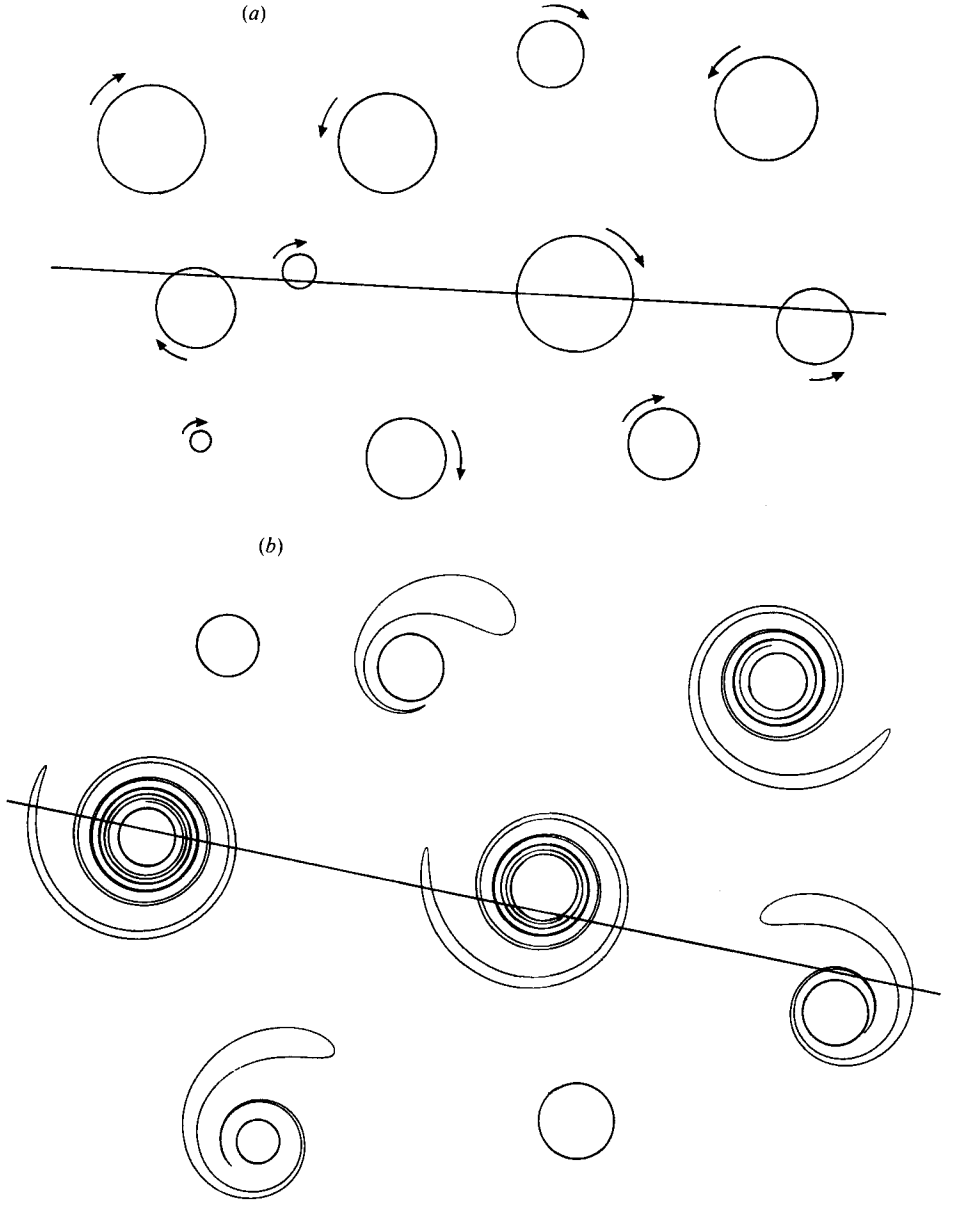


FIGURE 1. Two-dimensional turbulence as a collection of (*a*) coherent vortices (*b*) coherent vortices with spirals.

quasi-equilibrium three-dimensional turbulence. In §4, we examine models for decaying two-dimensional turbulence in which the vorticity is concentrated in vortices with spirals (figure 1*b*). We relate our calculations to some results concerning fractals, and briefly extend our view to a class of models employing self-similarity, filaments within filaments of the spiral, as might occur from several vortex collisions; these too have an energy spectrum of between $k^{-4}$ and $k^{-3}$.

## 2. The wind-up of a weak vortex patch by a strong vortex

We begin by applying the methods discussed in Moffatt (1984) to a simple model, the wind-up of the semi-infinite vortex patch shown in figure 2(*a*). This unsophisticated model is developed here to illustrate our methods of calculation so as to ease our examination of more complicated models. The vorticity, $\omega$, is unity inside the region $\mathscr{D}(t)$, and is zero outside. It is physically reasonable to take a discontinuous distribution of vorticity, since large gradients of vorticity are generated both in the formation of vortices and in the winding-up process. We treat the vorticity as a passive scalar advected by the flow of a point vortex of strength $2\pi^2\Gamma$, placed at $O$. Let $\epsilon$ be the distance from the patch to the vortex and let there be no viscous diffusion, $\nu = 0$. We use both polar coordinates $(r, \theta)$ and Cartesian coordinates $(x, y)$.

After some time $t$, the patch becomes filamented and wound round the vortex (figure 2*b*). A particle at $(r_0, \theta_0)$ when $t = 0$, now lies at

$$r(t) = r_0, \tag{2.1}$$

$$\theta(t) = \pi\Gamma t/r_0^2 + \theta_0, \tag{2.2}$$

and so the boundary of the patch, $\partial\mathscr{D}(t)$, is two spirals,

$$\theta(t) = \pi\Gamma t/r^2, \tag{2.3}$$

$$\theta(t) = \pi\Gamma t/r^2 + \pi, \tag{2.4}$$

for $r \geqslant \epsilon$, and a semicircle of radius $\epsilon$.

Let us examine the distribution of vorticity, $\omega_1(x)$, along the line $y = 0$, which cuts through the vortex. Now $\omega_1(x)$ has discontinuities wherever $\partial\mathscr{D}(t)$ crosses the line $y = 0$, that is, at points $\pm x_n$, given by

$$x_n = (\Gamma t/n)^{\frac{1}{3}}, \tag{2.5}$$

with $1 \leqslant n \leqslant n_\epsilon \equiv \Gamma t/\epsilon^2$. The spacing between the discontinuities is given by

$$\Delta x_n \equiv |x_n - x_{n-1}| \sim (\Gamma t/n^3)^{\frac{1}{2}}, \tag{2.6}$$

where we neglect constants of order unity here and from now on. The distribution of these discontinuities gives us information about the Fourier transform of vorticity along the line $y = 0$,

$$\hat{\omega}_1(k) = \frac{1}{2\pi}\int \omega_1(x)\, \mathrm{e}^{-\mathrm{i}kx}\, \mathrm{d}x. \tag{2.7}$$

We shall concentrate on the contributions to $\hat{\omega}_1(k)$ from the discontinuities in $x > 0$, to avoid undue cancellation in this artificially symmetrical model. We shall also neglect the contribution from the point vortex for the time being. Thus we have

$$\hat{\omega}_1(k) \sim \frac{1}{k}\sum_{n=1}^{n_\epsilon} (-1)^n\, \mathrm{e}^{-\mathrm{i}kx_n}. \tag{2.8}$$

Now consider the Fourier transform for different ranges of $k$ (figure 3*a*).

(*a*) When the wavelength $1/k$ is short compared with the width of the finest filaments, $\epsilon^3/\Gamma t$, the Fourier transform resolves a series of separated discontinuities and we expect that $\hat{\omega}_1(k) \sim k^{-1}$. Indeed, since $k\Delta x_n \gtrsim 1$ in this range, $k\hat{\omega}_1(k)$ is, in practice, a sum of $n_\epsilon$ uncorrelated complex numbers of unit modulus. This can be

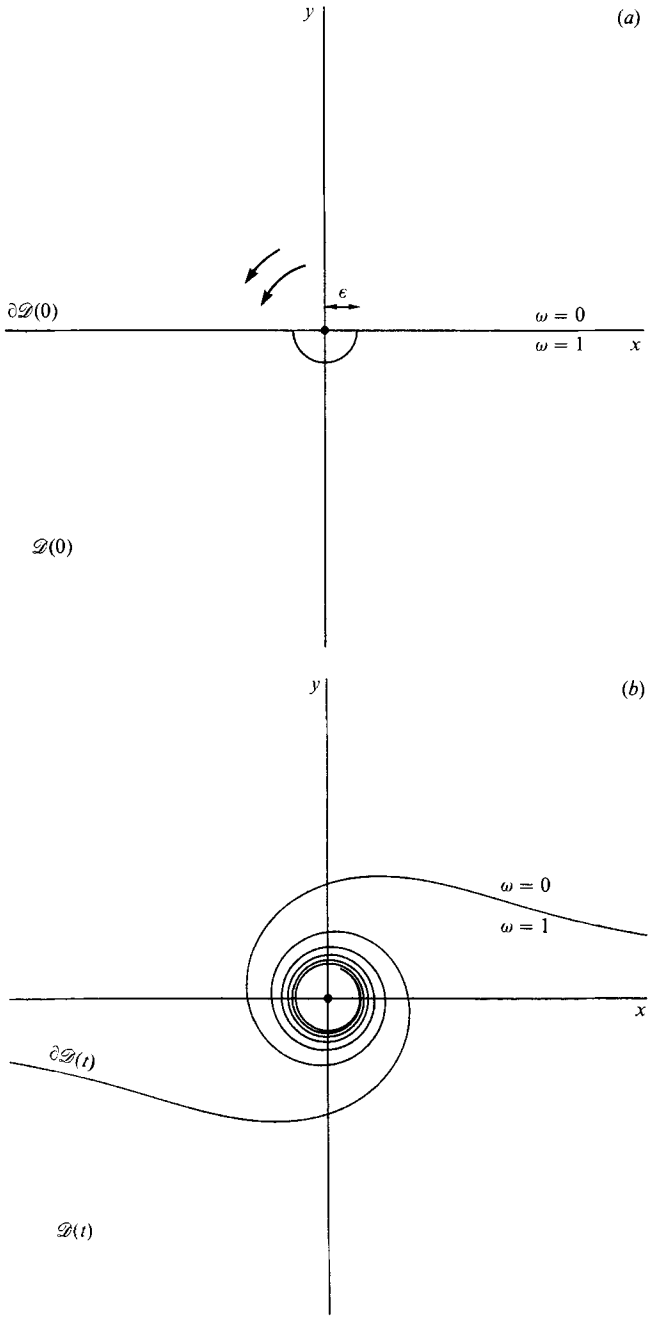


FIGURE 2. The configuration of a semi-infinite vortex patch (*a*) initially, at $t = 0$, (*b*) at a later time.

thought of as a random walk on the complex plane, and the mean-square distance from the start of the walk is simply the number of steps, which gives

$$|\hat{\omega}_1(k)| \sim n_\epsilon^{\frac{1}{2}} k^{-1} = (\Gamma t/\epsilon^2)^{\frac{1}{2}} k^{-1}. \tag{2.9}$$

This requires careful interpretation as a root-mean-square average over nearby values of $k$, since $\hat{\omega}_1(k)$ is a rapidly fluctuating function of $k$.

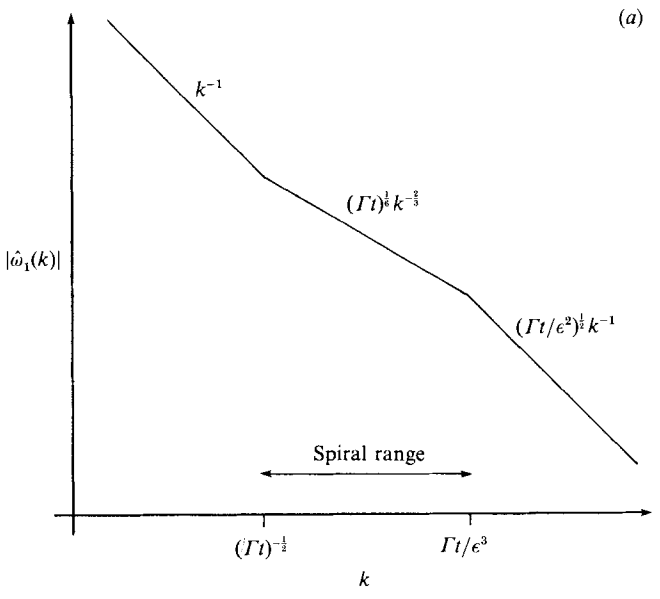


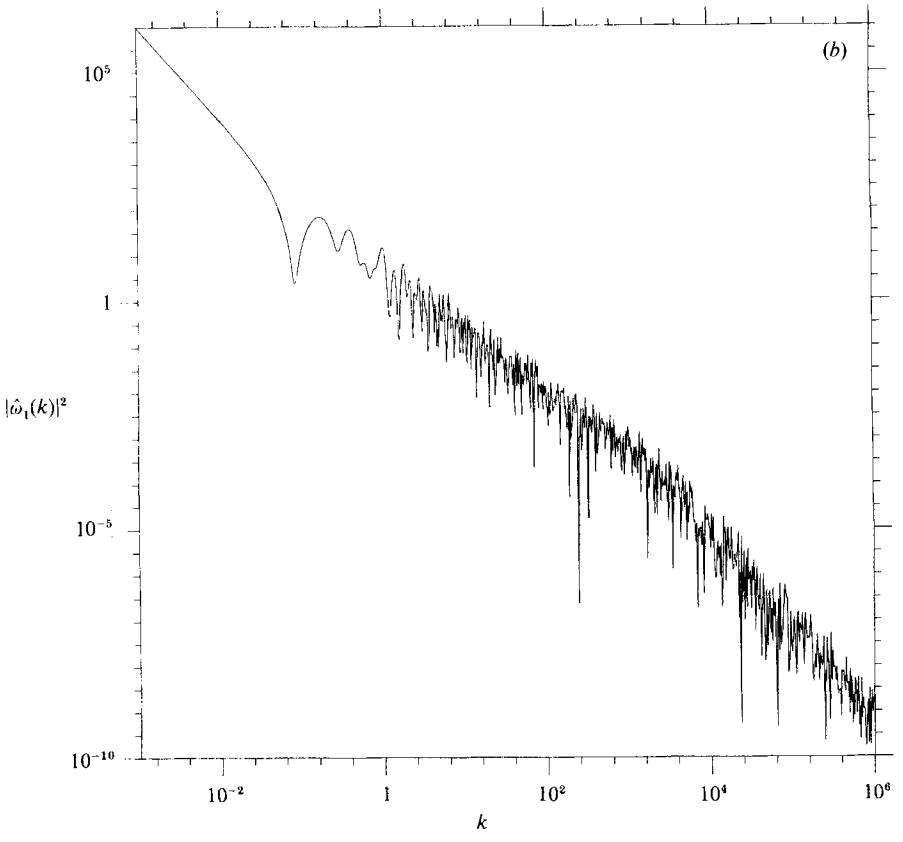


FIGURE 3(*a*, *b*). For caption see facing page.

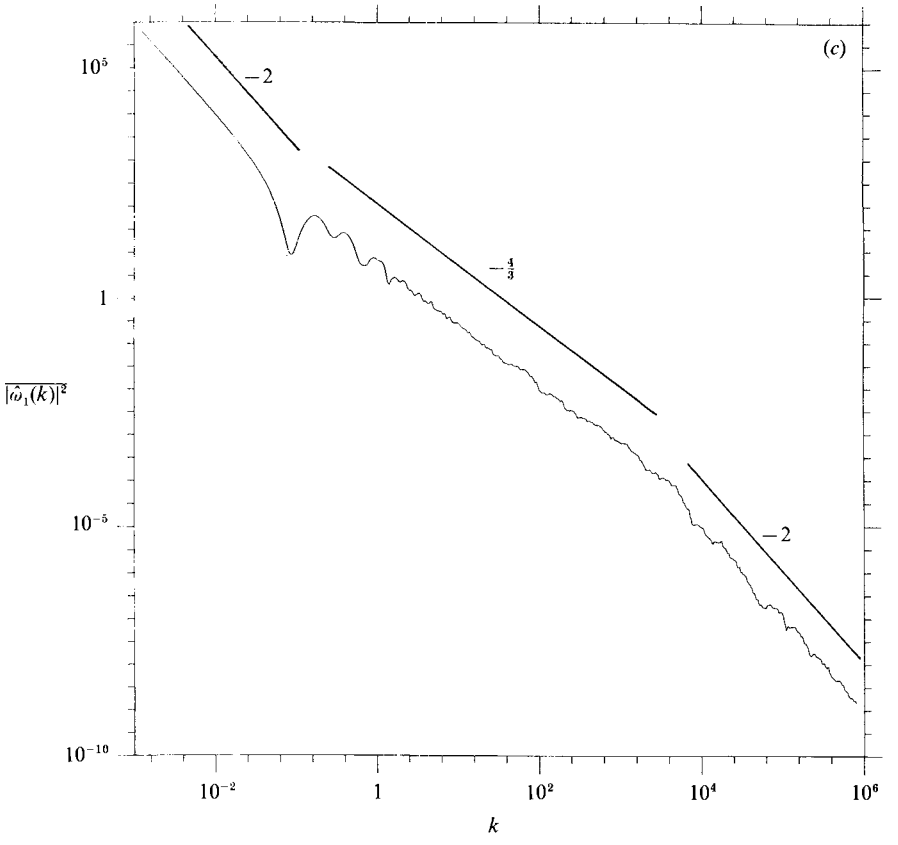


FIGURE 3. (*a*) Fourier transform, $|\hat{\omega}_1(k)|$, of the distribution of vorticity along $y = 0$ for the wind-up of a semi-infinite vortex patch. (*b*) Log–log plot of $|\hat{\omega}_1(k)|^2$ against $k$ for $\epsilon = 1$ and $\Gamma t = 1001$, calculated from equation (2.8). There are a hundred divisions per decade of $k$. (*c*) Log–log plot of the moving average of (*b*) over a fifth of a decade of $k$.

(*b*) For wavelengths $1/k$ between the width of the finest filaments, $\epsilon^3/\Gamma t$, and the width of the widest filaments, $(\Gamma t)^{\frac{1}{2}}$, the Fourier transform only resolves those discontinuities spaced by more than about a wavelength, $\Delta x_n \gtrsim 1/k$, that is, $1 \leqslant n \lesssim n_k \equiv (\Gamma t k^2)^{\frac{1}{3}}$. The dominant contribution to the Fourier transform is given by

$$\hat{\omega}_1(k) \sim \frac{1}{k} \sum_{n=1}^{n_k} (-1)^n \, \mathrm{e}^{-\mathrm{i}kx_n}. \tag{2.10}$$

This is effectively a sum of $n_k$ uncorrelated terms, yielding

$$|\hat{\omega}_1(k)| \sim n_k^{\frac{1}{2}} k^{-1} = (\Gamma t)^{\frac{1}{6}} k^{-\frac{2}{3}}, \tag{2.11}$$

which again is to be interpreted as an average behaviour. When $n$ is in the range $n_k \lesssim n \leqslant n_\epsilon$, the quantity $\mathrm{e}^{-\mathrm{i}kx_n}$ varies slowly with $n$ (as $k\Delta x_n \lesssim 1$); the terms tend to cancel because of the factor, $(-1)^n$, and their contribution to $k\hat{\omega}_1(k)$ is of order unity and so negligible.† We can picture these wavelengths as seeing an *accumulation point* of discontinuities. This is a worse singularity than simply a number of separated discontinuities and so leads to a slower fall-off of $k^{-\frac{2}{3}}$ in the Fourier transform. For

† There is an error in Moffatt (1984) at this point. It is stated that the terms with $kx_n \lesssim 1$ are negligible. However it is the *spacing*, $\Delta x_n$, between the discontinuities that is important, not the distance, $x_n$.

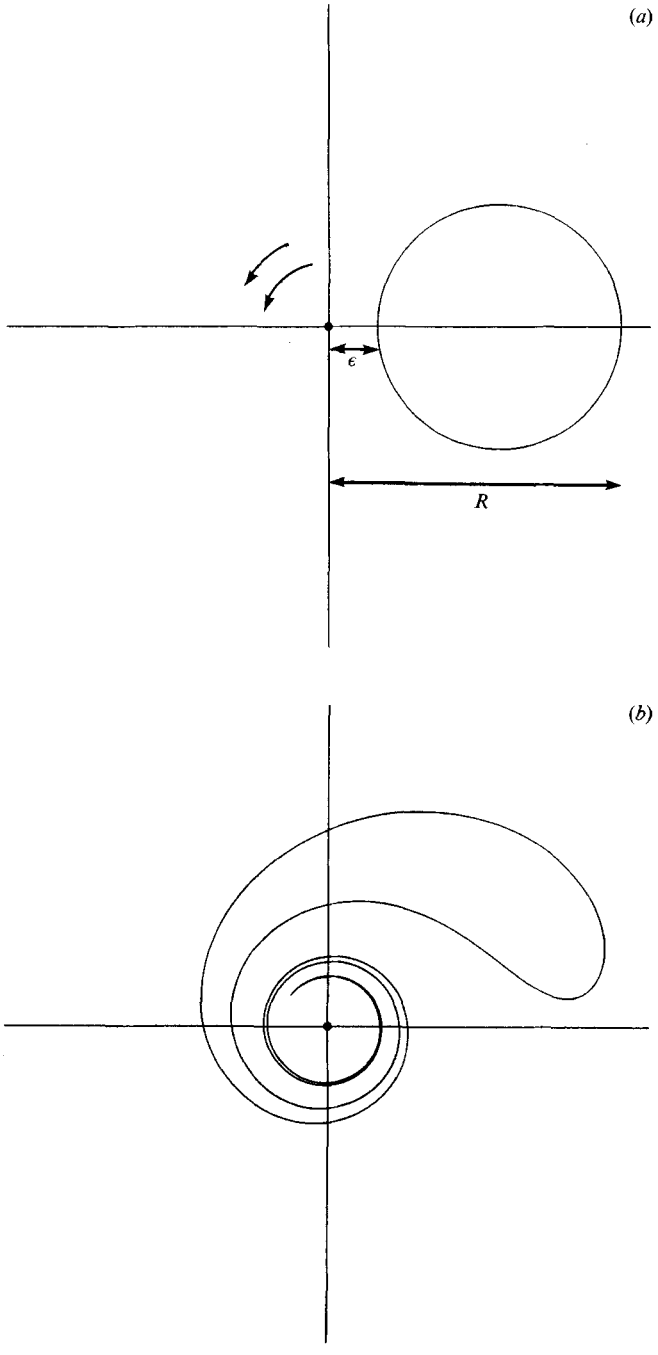


FIGURE 4(a, b). For caption see facing page.

brevity, let us coin the term 'spiral range' for a range of $k$ such as this, in which a spiral accumulation of discontinuities leads to a slow fall-off in the Fourier transform, $\hat{\omega}_1(k)$.

(c) On scales greater than the width of any filament, $1/k \gtrsim (\Gamma t)^{\frac{1}{2}}$, the Fourier transform resolves none of the spiral structure and just sees a semi-infinite patch.

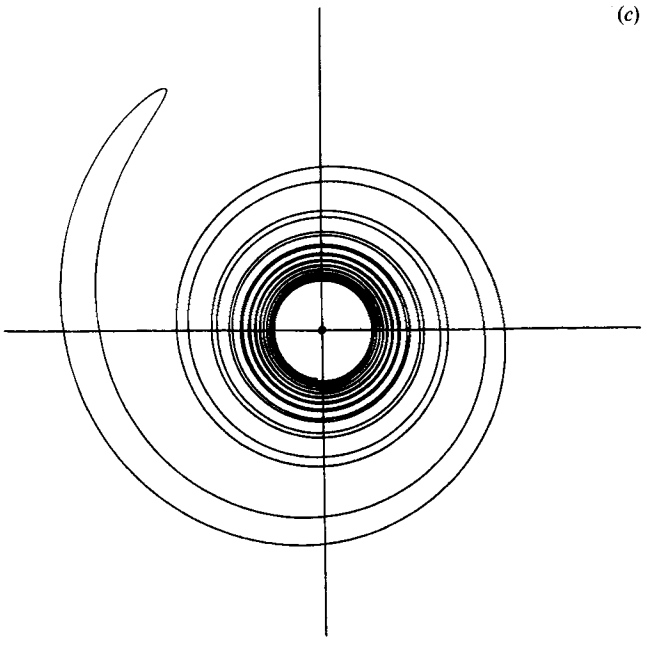


FIGURE 4. Configuration of a finite vortex patch for times $t$, with (*a*) $0 \lesssim \Gamma t \lesssim \epsilon^s$, (*b*) $\epsilon^s \lesssim \Gamma t \lesssim R^s$, (*c*) $R^s \lesssim \Gamma t$.

The terms $e^{-ikx_n}$ vary slowly with $n$, and the sum is of order unity, so that

$$|\hat{\omega}_1(k)| \sim k^{-1}. \tag{2.12}$$

We have demonstrated that this simple model gives the Fourier transform shown schematically in figure 3(*a*). The spiral gives rise to the range with the $k^{-\frac{2}{3}}$ fall-off in $\hat{\omega}_1(k)$, and the presence of discontinuities gives two ranges with a $k^{-1}$ fall-off. This may be compared with the numerical results shown in figure 3(*b*), in which $|\hat{\omega}_1(k)|^2$ is calculated from (2.8) for $\epsilon = 1$ and $\Gamma t = 1001$. Figure 3(*c*) shows a moving average of figure 3(*b*); this smooths out the rapid variations of $|\hat{\omega}_1(k)|^2$ (figure 3*b* does not resolve all the fine structure here). There is a good agreement with the above calculations (up to constants of order one). Note that we have assumed that there is a good separation of scales; we shall take this for granted in further calculations and diagrams.

We now refine the above model to the case of a patch, $\mathscr{D}(t)$, with smooth boundary and finite radius, $R$ (figure 4*a*). We still treat the patch as a passive scalar without viscous diffusion but now we generalize the velocity field to

$$\dot{r} = 0, \tag{2.13}$$

$$\dot{\theta} = \pi\Gamma/r^s. \tag{2.14}$$

For a point vortex, $s = 2$; however this generalization might be useful to include some average axisymmetric effect of the patch on the velocity field. The calculations are similar to those we have presented for the semi-infinite patch, and we shall omit uninteresting details.

For short times, $0 \lesssim t \lesssim \epsilon^s/\Gamma$, before the patch becomes wound round the vortex (figure 4*a*), Saffman's (1971) argument applies, and thus

$$|\hat{\omega}_1(k)| \sim \begin{cases} R, & k \lesssim 1/R \\ k^{-1}, & k \gtrsim 1/R \end{cases}. \tag{2.15}$$

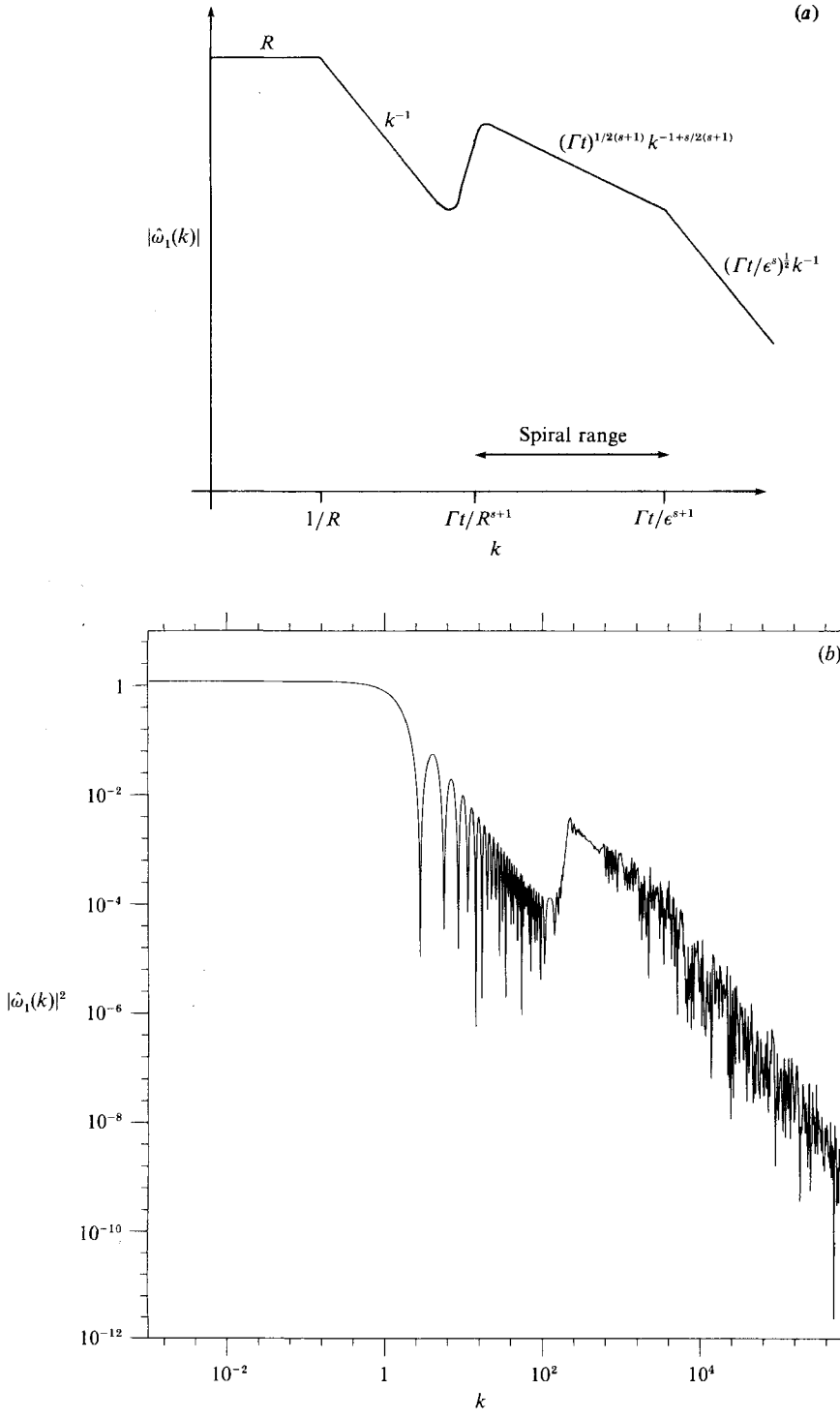


FIGURE 5(*a*, *b*). For caption see facing page.

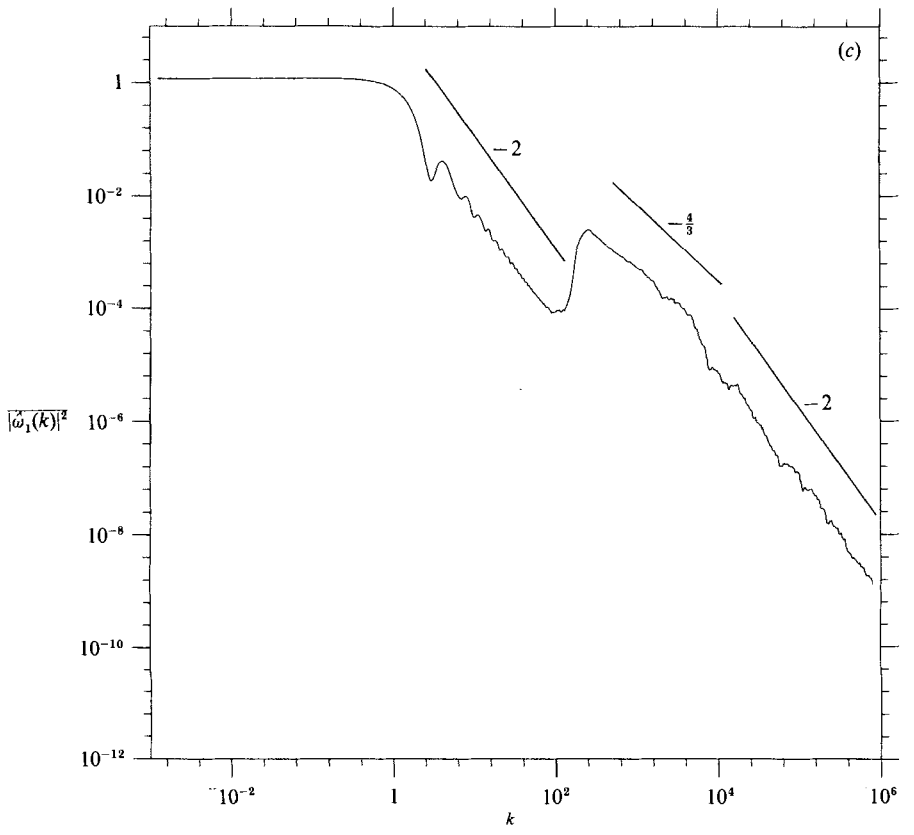


FIGURE 5. (*a*) Fourier transform, $|\hat{\omega}_1(k)|$, of the distribution of vorticity along $y = 0$ for the wind-up of a finite patch, at times with $\Gamma t \gtrsim R^s$. (*b*) Log–log plot of $|\hat{\omega}_1(k)|^2$ against $k$ for $n_e = 1001$, $n_R = 100$, $\Gamma t = 1001$ and $s = 2$, calculated from equation (2.19). There are a hundred divisions per decade of $k$. (*c*) Log–log plot of the moving average of (*b*) over a fifth of a decade of $k$.

For times $t$ with $\epsilon^s \lesssim \Gamma t \lesssim R^s$, the vortex has wound the closest part of the patch into a spiral, but this filamentation process has yet to affect the far edge of the patch (figure 4*b*). We again have discontinuities in $\omega_1(x)$ at points $x_n$, where $\partial\mathscr{D}(t)$ crosses $y = 0$. The detailed distribution of these points depends on the initial shape of the patch; however to calculate $\hat{\omega}_1(k)$ we need only know the rate of accumulation of these discontinuities. We assume that initially the boundary of the patch, $\partial\mathscr{D}(0)$, is smooth, and does not possess structure on scales smaller than $R$. Then any small piece of the boundary will be stretched into a spiral round the vortex and so will accumulate at a rate *independent* of its initial angle, $\theta$, and initial orientation. This rate of accumulation may be calculated as before, yielding

$$x_n \sim (\Gamma t/n)^{1/s}, \tag{2.16}$$

$$\Delta x_n \sim (\Gamma t/n^{s+1})^{1/s}, \tag{2.17}$$

with $1 \leqslant n \leqslant n_e \equiv \Gamma t/\epsilon^s$, and the Fourier transform of the vorticity distribution along $x = 0$ is given by

$$|\hat{\omega}_1(k)| \sim \begin{Bmatrix} R, & 0 \lesssim k \lesssim 1/R \\ k^{-1}, & 1/R \lesssim k \lesssim (\Gamma t)^{-1/s} \\ (\Gamma t)^{1/2(s+1)}\, k^{-1+s/2(s+1)}, & (\Gamma t)^{-1/s} \lesssim k \lesssim \Gamma t/\epsilon^{s+1} \\ (\Gamma t/\epsilon^s)^{\frac{1}{2}} k^{-1}, & \Gamma t/\epsilon^{s+1} \lesssim k. \end{Bmatrix} \tag{2.18}$$

The first range of $k$ consists of long wavelengths which do not resolve the size of the patch. In the second range the Fourier transform resolves the patch, but none of the spiral. Wavelengths in the third (spiral) range see an accumulation point of discontinuities, and, finally, short wavelengths resolve the spiral structure completely.

At later times with $\Gamma t \gtrsim R^s$ the whole patch is wound into a spiral by the central vortex (figure 4c). Now discontinuities only occur for $n_R \equiv \Gamma t/R^s \leqslant n \leqslant n_\epsilon \equiv \Gamma t/\epsilon^s$ and the Fourier transform, given by

$$\hat{\omega}_1(k) \sim \frac{1}{k} \sum_{n_R}^{n_\epsilon} (-1)^n \, \mathrm{e}^{-\mathrm{i}kx_n}, \tag{2.19}$$

is shown in figure 5(a). When $k$ is in the spiral range, $\Gamma t/R^{s+1} \lesssim k \lesssim \Gamma t/\epsilon^{s+1}$, the Fourier transform sees an accumulation point of discontinuities. It only resolves those spaced by more than a wavelength, that is, those with $n_R \leqslant n \lesssim n_k \equiv (\Gamma t k^s)^{1/(s+1)}$. These give a sum of uncorrelated terms, while the remaining unresolved discontinuities give a contribution of order unity, so that

$$|\hat{\omega}_1(k)| \sim k^{-1}[(n_k - n_R)^{\frac{1}{2}} + O(1)]. \tag{2.20}$$

Thus at $k \sim \Gamma t/R^{s+1}$ there is a rapid rise in the Fourier transform, as new structure is resolved; this is a consequence of the finite size of the patch, and did not occur in the example of the semi-infinite patch considered earlier. For $\Gamma t/R^{s+1} \lesssim k \lesssim \Gamma t/\epsilon^{s+1}$ we have the slow fall-off in the spiral range:

$$|\hat{\omega}_1(k)| \sim (\Gamma t)^{1/2(s+1)} \, k^{-1+s/2(s+1)}. \tag{2.21}$$

These calculations of the Fourier transform are confirmed by numerical results (figure 5b, c).

Let us introduce weak viscous diffusion of the vortex patch, $\nu \neq 0$. This smooths out vorticity on the lengthscale $(\nu t)^{\frac{1}{2}}$, which increases with time. The effect of viscosity is to diffuse away filaments with width less than this viscous lengthscale. This modifies the evolution of a vortex patch; first the innermost filaments diffuse away and eventually the vorticity distribution becomes axisymmetric. Precisely when these processes occur depends on how the viscous lengthscale compares with the other scales in the problem. In Fourier space the picture is simpler; viscous diffusion gives rise to an exponential decay of $\hat{\omega}_1(k)$ at small scales, $k \geqslant 1(\nu t)^{\frac{1}{2}}$.

We now consider the vortex core causing the advection of the patch; plainly a point vortex is physically unrealistic and would dominate the energy spectrum at all wavelengths. In our model we shall replace it by a smooth axisymmetric vorticity distribution of lengthscale $\epsilon$, for example

$$\omega(x, y) = (\pi\Gamma/\epsilon^2) \, \mathrm{e}^{-(x^2+y^2)/2\epsilon^2}, \tag{2.22}$$

$$\omega_1(x) = (\pi\Gamma/\epsilon^2) \, \mathrm{e}^{-x^2/2\epsilon^2}, \tag{2.23}$$

$$\hat{\omega}_1(k) = (\Gamma/\epsilon)(\pi/2)^{\frac{1}{2}} \, \mathrm{e}^{-\epsilon^2 k^2/2}. \tag{2.24}$$

The distribution decays exponentially for $k \gtrsim 1/\epsilon$, but dominates the Fourier transform when $k \lesssim 1/\epsilon$, since the condition that the vortex patch is weak compared with the vortex core is

$$\Gamma \gg R^2. \tag{2.25}$$

This modifies the forms of $\hat{\omega}_1(k)$ that we have calculated; also the viscous diffusion of the core will affect the late stages of evolution of the patch. Note that we could

take a smooth axisymmetric vortex core of radius larger than $O(\epsilon)$, and investigate the wind-up of *superposed* variations in vorticity, here modelled as a vortex patch.

The calculations of $\hat{\omega}_1(k)$, without viscosity and excluding the vorticity of the central vortex, are valid for $1/\epsilon \lesssim k \lesssim 1/(\nu t)^{\frac{1}{2}}$. To include these effects, we need only introduce an exponential decay for $k \gtrsim 1/(\nu t)^{\frac{1}{2}}$ and a distribution such as (2.24) for $k \lesssim 1/\epsilon$.

## 3. Calculation of the energy spectrum

In this section we show how the energy spectrum $E(k)$ of a vortex with a spiral may be calculated from the Fourier transform of the vorticity along lines cutting through the vortex; we also confirm these calculations by the method of Lundgren (1982).

We have examined the Fourier transform $\hat{\omega}_1(k)$ of vorticity along a line $y = 0$, passing through the very centre of the spiral. However such a line is unrepresentative for the purposes of calculating the energy spectrum; therefore let $\hat{\omega}_1(k; y_0)$ be the Fourier transform of the vorticity distribution $\omega(x, y_0)$ along the line $y = y_0$. Define $\phi(k)$ by (Saffman 1971)

$$\int \omega(x,y)\,\omega(x+\xi,y)\,\mathrm{d}x\,\mathrm{d}y = \int \phi(k)\,\mathrm{e}^{\mathrm{i}k\xi}\,\mathrm{d}k; \tag{3.1}$$

then

$$\phi(k) = 2\pi \int |\hat{\omega}_1(k;y)|^2\,\mathrm{d}y. \tag{3.2}$$

Consider a spiral wrapped around some vortex core. Within our policy of neglecting constants of order unity, such a structure is isotropic (all directions are approximately the same) but not homogeneous (not all points are the same). Using isotropy, $\phi(k)$ may be related to $E(k)$ (Saffman 1971) by

$$\phi(k) = \frac{1}{\pi}\int_{-\infty}^{\infty} (k^2+l^2)^{\frac{1}{2}} E[(k^2+l^2)^{\frac{1}{2}}]\,\mathrm{d}l \tag{3.3}$$

with inverse

$$k^3 E(k) = \int_k^{\infty} \frac{-l}{(l^2-k^2)^{\frac{1}{2}}} \frac{\mathrm{d}}{\mathrm{d}l}[l\phi(l)]\,\mathrm{d}l. \tag{3.4}$$

We calculate the energy spectrum from $\phi(k)$ by (3.4), and find $\phi(k)$ by integrating $|\hat{\omega}_1(k; y_0)|^2$ over parallel lines $y = y_0$. In the ranges in which $k\hat{\omega}_1(k; y_0)$ is a rapidly varying sum of uncorrelated terms, this integration will smooth out the fluctuations, leaving us with the mean-square behaviour.

We need to modify the calculations of §2 for the case of a line $y = y_0$ intersecting the vortex. We shall neglect viscosity and the vorticity of the vortex core; when we include these, our results will remain valid in the range $1/\epsilon \lesssim k \lesssim 1/(\nu t)^{\frac{1}{2}}$. Consider, for example, the vortex shown in figure 4(*c*); here the whole patch has become wound up into a spiral. Take a line $y = y_0$ through the vortex; the vorticity distribution along the line, $\omega(x, y_0)$, possesses discontinuities at $x_n$, where

$$x_n \sim [(\Gamma t/n)^{2/s} - y_0^2]^{\frac{1}{2}} \sim (\Gamma t/n)^{1/s}, \tag{3.5}$$

with $n_R \leqslant n \leqslant \min(n_\epsilon, n_{y_0})$ and $n_{y_0} \equiv \Gamma t/y_0^s$. We can calculate the mean behaviour of $|\hat{\omega}_1(k; y)|^2$ for a given $y$ by the methods used in §2. Integrating these results over $y$ gives $\phi(k)$, which decays as $(\Gamma t)^{2/(s+1)} k^{-2+(s-1)/(s+1)}$ in the spiral range, $\Gamma t/R^{s+1} \lesssim$

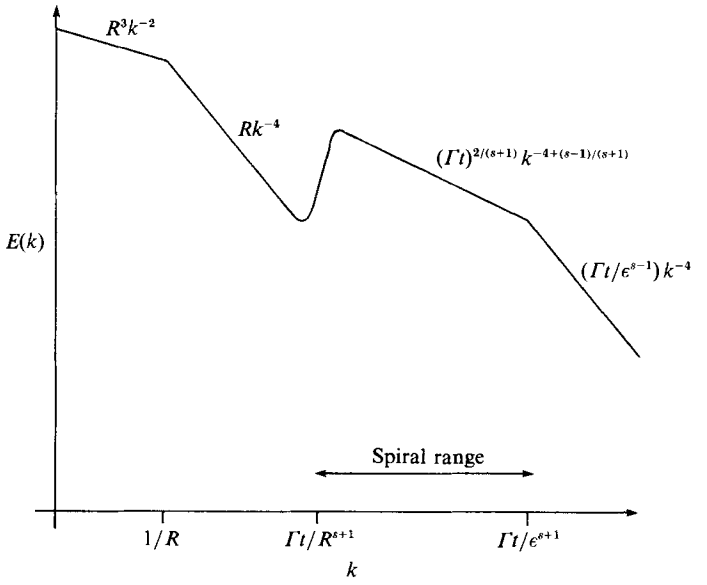


FIGURE 6. The energy spectrum for a spiral with $\Gamma t \gtrsim R^s$; the contribution of the vortex core and the effect of viscosity are not shown.

$k \lesssim \Gamma t/\epsilon^{s+1}$. Note that the integration means that $\phi(k)$ has a different power-law dependence on $k$ from $|\hat{\omega}_1(k)|^2$ in this range.

The energy spectrum of the vortex, $E(k)$, is displayed in figure 6. In the spiral range the energy has been modified from the $k^{-4}$ characteristic of separated discontinuities (Saffman 1971), to a $k^{-4+(s-1)/(s+1)}$ spectrum. We have assumed $s > 1$ in the above calculations; spirals with $s < 1$ are too loosely coiled to change the spectrum from $k^{-4}$. As $s$ varies from one to infinity, the power law varies from $k^{-4}$ to $k^{-3}$. We expect that $s \approx 2$ for a realistic model of the wind-up of a weak vortex patch by a strong vortex; when $s = 2$ as in the point-vortex model of §2, this is a $k^{-11/3}$ spectrum. We have calculated the energy spectrum for times $t \gtrsim R^s/\Gamma$, when the whole patch is filamented; it can also be calculated for earlier times. For $\Gamma t \lesssim R\epsilon^{s-1}$ the spiral gives a negligible contribution to the energy spectrum, $Rk^{-4}$; only when $\Gamma t \gtrsim R\epsilon^{s-1}$ does a spiral range emerge.

We now show how the energy spectrum may be calculated by the methods used in Lundgren (1982). We work in polar coordinates $(r, \theta)$ in this section. We consider a patch of vorticity $\omega(r, \theta)$ advected in the flow with angular velocity $\dot{\theta}(t) \equiv \Omega(r) = \Gamma/r^s$, caused by some axisymmetric vortex core at $O$ of radius $\epsilon$, as in §2. The advection of the patch is given by

$$\frac{\mathrm{D}\omega}{\mathrm{D}t} = \frac{\partial \omega}{\partial t} + \Omega(r)\frac{\partial \omega}{\partial \theta} = 0. \tag{3.6}$$

This equation is easily seen to have the general solution

$$\omega(r, \theta, t) = \sum_{n=-\infty}^{\infty} f_n(r)\, \mathrm{e}^{\mathrm{i}n\theta - \mathrm{i}n\Omega t}, \tag{3.7}$$

corresponding to a general initial condition

$$\omega(r, \theta, 0) = \sum_{n=-\infty}^{\infty} f_n(r)\, \mathrm{e}^{\mathrm{i}n\theta}. \tag{3.8}$$

The functions $f_n(r)$ must satisfy $f_n(r) = f^*_{-n}(r)$ to make $\omega$ real. Also, we include the vortex core in $f_0(r)$ which must vanish for $r > R$; for $n \neq 0$, $f_n(r)$ must vanish for $r < \epsilon$ or $r > R$.

The effect of viscosity is to modify (3.6) to

$$\frac{\mathrm{D}\omega}{\mathrm{D}t} = \frac{\partial\omega}{\partial t} + \Omega(r)\frac{\partial\omega}{\partial\theta} = \nu\nabla^2\omega, \tag{3.9}$$

with approximate solution (Lundgren 1982)

$$\omega(r,\theta,t) \approx \sum_{n=-\infty}^{\infty} f_n(r)\,\mathrm{e}^{\mathrm{i}n\theta - \mathrm{i}n\Omega t}\,\mathrm{e}^{-n^2\Omega'^2\nu t^3/3}. \tag{3.10}$$

The non-zero harmonics decay on timescales $t_\nu \lesssim (R^2/\nu\Omega^2)^{\frac{1}{3}}$, while the zero harmonic can be shown (Lundgren 1982) to decay on the much longer timescale $t_{\nu 0} = R^2/\nu$. The ratio is $t_{\nu 0}/t_\nu \gtrsim Re^{\frac{2}{3}}$ and we take the Reynolds number, based on the scales of the vortex, $Re \equiv R^2\Omega/\nu$, to be large. The differential rotation due to the vortex core winds up the vorticity into a spiral and increases the vorticity gradients, which enhances the decay of non-zero harmonics. This process is precisely analogous to the expulsion of the flux of a magnetic field from a region of a two-dimensional fluid with closed streamlines (Weiss 1966; Moffatt & Kamkar 1983; Rhines & Young 1983). In this case the vector potential of the magnetic field is advected by the fluid flow and its diffusion is enhanced by differential rotation in the same way.

We use the Fourier transform pair:

$$\omega(\boldsymbol{r}) = \int \hat{\omega}(\boldsymbol{k})\,\mathrm{e}^{\mathrm{i}\boldsymbol{k}\cdot\boldsymbol{r}}\,\mathrm{d}^2\boldsymbol{k}, \tag{3.11}$$

$$\hat{\omega}(\boldsymbol{k}) = (2\pi)^{-2}\int \omega(\boldsymbol{r})\,\mathrm{e}^{-\mathrm{i}\boldsymbol{k}\cdot\boldsymbol{r}}\,\mathrm{d}^2\boldsymbol{r}. \tag{3.12}$$

The energy spectrum is given by

$$E(k) = \frac{2\pi^2}{k}\int |\hat{\omega}(\boldsymbol{k})|^2\,\mathrm{d}\theta_k, \tag{3.13}$$

where $\boldsymbol{k} = (k, \theta_k)$ in polar coordinates. Substituting for $\omega(\boldsymbol{r})$ from (3.10), we obtain

$$\hat{\omega}(\boldsymbol{k}) = \frac{1}{2\pi}\sum_{n=-\infty}^{\infty}(-\mathrm{i})^n I_n(k)\,\mathrm{e}^{\mathrm{i}n\theta_k}, \tag{3.14}$$

$$E(k) = \frac{\pi}{k}\left[I_0(k)^2 + 2\sum_{n=1}^{\infty}|I_n(k)|^2\right], \tag{3.15}$$

where

$$I_n(k) \equiv \int_0^\infty J_n(kr) f_n(r)\,\mathrm{e}^{-\mathrm{i}n\Omega t}\,\mathrm{e}^{-n^2\Omega'^2\nu t^3/3}\,r\,\mathrm{d}r. \tag{3.16}$$

Now $f_n(r)$ is zero for $r < \epsilon$ and $n \neq 0$; so for wavenumbers $k \gtrsim 1/\epsilon$ we can use the asymptotic expansion for the Bessel functions

$$J_n(kr) \sim (2\pi kr)^{-\frac{1}{2}}[(-\mathrm{i})^{n+\frac{1}{2}}\mathrm{e}^{\mathrm{i}kr} + \mathrm{i}^{n+\frac{1}{2}}\mathrm{e}^{-\mathrm{i}kr}] \tag{3.17}$$

and approximate the integral (3.16) by the method of stationary phase. The exponential is stationary at $r = r_n$ with, for $n > 0$,

$$r_n = (ns\Gamma t/k)^{1/(s+1)}. \tag{3.18}$$

This gives a contribution to $I_n(k)$ provided $\epsilon < r_n < R$ so that $f_n(r_n) \neq 0$. If we assume that there is such a contribution, and that it dominates the contributions from the endpoints, $r = \epsilon$ and $r = R$, of the integral (3.16), we obtain

$$I_n(k) \approx \left[\frac{r_n}{nk\Omega''(r_n)t}\right]^{\frac{1}{2}} \mathrm{i}^n f_n(r_n)\, \mathrm{e}^{-\mathrm{i}kr_n - \mathrm{i}n\Omega(r_n)t} \mathrm{e}^{-n^2\Omega'(r_n)^2\nu t^3/3} \tag{3.19}$$

and

$$E(k) = \frac{\pi}{k}\left[I_0(k)^2 + 2\sum_{n=1}^{\infty} \frac{r_n^{s+3}}{ns(s+1)\,k\Gamma t} |f_n(r_n)|^2\, \mathrm{e}^{-2\nu k^2 t/3}\right]. \tag{3.20}$$

Now $I_0$ contains contributions from the zero harmonic of the spiral and from the vortex core. If we take the core to be a smooth distribution of vorticity of lengthscale $\epsilon$, then as before this dominates the spectrum for $k \lesssim 1/\epsilon$ but may be ignored outside this range. For the zero harmonic, the phase is never stationary and the endpoints of the integral (3.16) give the dominant contribution, which we are assuming is negligible compared with the stationary phase contributions from other harmonics.

Let us investigate the spectrum in the range $1/\epsilon \lesssim k \lesssim 1/(\nu t)^{\frac{1}{2}}$, and drop all multiplicative constants of order unity (including $s$). In this range

$$E(k) \sim k^{-3} \sum_{n=1}^{\infty} (n\Gamma t/k)^{2/(s+1)} |f_n(r_n)|^2. \tag{3.21}$$

We need only sum over those $n$ for which $f_n(r_n)$ is non-zero, that is, for which $\epsilon \lesssim r_n \lesssim R$ or

$$n_\ell \equiv k\epsilon^{s+1}/\Gamma t \lesssim n \lesssim kR^{s+1}/\Gamma t \equiv n_{\mathrm{u}}. \tag{3.22}$$

There are three distinct ranges of $k$:

(*a*) $k \lesssim \Gamma t/R^{s+1}$. In this range $n_\ell \lesssim n_{\mathrm{u}} \lesssim 1$, and there are no stationary phase contributions to the energy integral. Contributions come from the endpoints of the integral, giving rise to an energy spectrum proportional to $k^{-4}$.

(*b*) $\Gamma t/R^{s+1} \lesssim k \lesssim \Gamma t/\epsilon^{s+1}$. In this range $n_\ell \lesssim 1 \lesssim n_{\mathrm{u}}$ and so there are stationary phase contributions from the harmonics $n = 1$ to $n_{\mathrm{u}}$.

(*c*) $\Gamma t/\epsilon^{s+1} \lesssim k$. Here $1 \lesssim n_\ell \lesssim n_{\mathrm{u}}$ and harmonics $n = n_\ell$ to $n_{\mathrm{u}}$ give stationary phase contributions to the energy spectrum.

We shall calculate $E(k)$ for $k$ in the ranges (*b*) and (*c*) above. We need to assume more about the structure of $f_n(r)$ to do this. We are dealing with a vortex patch which, at $t = 0$, is without structure on scales much smaller than $R$. The harmonics $f_n(r)$ of the vorticity distribution will only depend weakly on $r$, and will vary as $1/n$, since the distribution is discontinuous. Thus we shall take $f_n \sim 1/n$ (independent of $r$) for $\epsilon < r < R$ and $n \neq 0$. In any case, we expect the spectrum to be approximately the same for any vortex patch that initially does not possess small-scale structure. In order to use (3.21) with this form of $f_n(r)$, we need to check that the contribution to $E(k)$ from the endpoints of the integrals in (3.16) is negligible compared with the stationary phase contribution. This is true when $k$ is in one of the ranges (*b*) or (*c*) above and $\Gamma t \gtrsim R^s$, so that the process of filamentation has reached the outer edge of the patch (figure 4*c*).

Thus in the range (*b*), with $\Gamma t \gtrsim R^s$,

$$E(k) \sim k^{-3} \sum_{n=1}^{n_{\mathrm{u}}} (n\Gamma t/k)^{2/(s+1)}\, n^{-2} \tag{3.23}$$

$$\approx k^{-3}(\Gamma t/k)^{2/(s+1)} \int_1^{n_{\mathrm{u}}} n^{-2+2/(s+1)}\, \mathrm{d}n \tag{3.24}$$

$$\sim (\Gamma t)^{2/(s+1)}\, k^{-4+(s-1)/(s+1)}. \tag{3.25}$$

Similarly in the range (*c*), with $\Gamma t \gtrsim R^s$,

$$E(k) \sim k^{-3}(\Gamma t/k)^{2/(s+1)} \int_{n_\ell}^{n_u} n^{-2+2/(s+1)}\,\mathrm{d}n \tag{3.26}$$

$$\sim (\Gamma t/\epsilon^{s-1})\,k^{-4}. \tag{3.27}$$

These results agree with those we found earlier (figure 6) by more physical arguments. Note that again we have assumed that $s > 1$; a spiral with $s < 1$ is too 'weak' a singularity to give an energy spectrum different from that of a discontinuity, $E(k) \sim k^{-4}$.

## 4. Models of two-dimensional turbulence

What implications do our calculations have for simple physical-space models of two-dimensional turbulence? Can the filamentation of vorticity by coherent vortices reconcile Saffman's (1971) $k^{-4}$ energy spectrum with the $k^{-3}$ spectrum suggested by cascade models? Let us work within the following picture of the later stages of decaying two-dimensional turbulence. The vorticity is mostly concentrated in coherent vortices which move in the velocity field they induce, and occasionally interact. The vortices acquire spirals either during their formation, through vortex instabilities, or by assimilating other vortices.

With this picture in mind, we model the fluid as containing a collection of vortices with spirals parameterized by values of $\Gamma, t, s, \epsilon$ and $R$. For scales smaller than the spacing between the vortices the energy spectrum is the sum of the spectra of the individual vortices. (At larger scales the distribution of the vortices is important. Models of the dynamics and interactions of vortices may throw some light on the predictions of a $k^{-\frac{5}{3}}$ energy spectrum in an up-scale energy cascade.) First let us note that coherent vortices are likely to acquire spiral structures during their formation, from the winding-up of variations in the initial vorticity distribution. If we assume these vortices and initial spirals have approximately the same structure and size, then the energy spectrum will contain a time-dependent $k^{-4+(s-1)/(s+1)}$ spiral range, as discussed in §§2 and 3.

At later times the vortices will continue to acquire further spirals created through vortex instabilities and collisions, and these will come to dominate the initial spirals, which will eventually diffuse away. This creation of further spirals around the coherent vortices suggests that the simplest model of two-dimensional turbulence we can construct is one in which new identical spirals are continually created and are destroyed after a time $t_c$. The only mechanism that can destroy the fine scales of a spiral is diffusion; thus we are led to assume that after a time $t_c$ an old spiral has already diffused into an axisymmetric distribution, and the vortex starts to develop a new spiral through a collision with another vortex. We also take $t_c$ short enough that the spirals do have a significant effect on the energy spectrum; so $t_c$ must satisfy

$$R^{s+1}(\nu t_c)^{-\frac{1}{2}} \lesssim \Gamma t_c \lesssim R^{s+4}(\nu t_c)^{-2}. \tag{4.1}$$

The energy spectrum, then, is proportional to that of a single vortex averaged over its lifetime $t_c$, and is shown in figure 7. We see that we have a range with a $k^{-4}$ spectrum, and a range with a decay of $k^{-2}$, which is the time-averaged effect of the spiral range with its promising $k^{-4+(s-1)/(s+1)}$ spectrum. This averaged $k^{-2}$ energy spectrum falls off very slowly for an inertial range, and makes this a rather unlikely model of decaying two-dimensional turbulence.

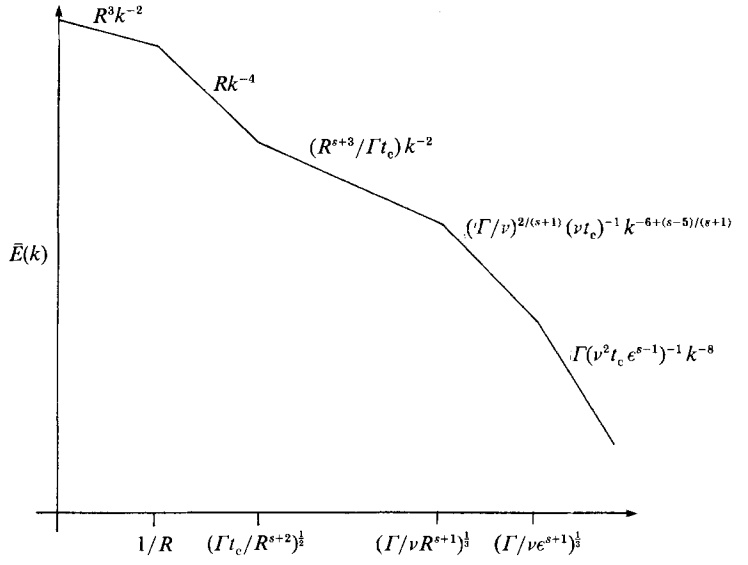


FIGURE 7. The energy spectrum of a single vortex averaged over its lifetime, $t_c$. Viscosity is included, but not the contribution from the vortex core.

We could, of course, obtain any desired spectrum by making arbitrary assumptions about the distribution of vortices with different values of $\Gamma, s, \epsilon, R$ and lifetime $t_c$. However, the main problem with our model is the assumption that spirals survive until they are destroyed by viscosity. Consider the inviscid limit; as $\nu \to 0$, the time taken for the spirals to diffuse away tends to infinity but the large-scale dynamics, which comprise the motion and interactions of vortices, will be independent of viscosity in this limit. Thus for small viscosity, we expect that a spiral will be disrupted by a close encounter with another vortex, long before it has diffused away. The encounter will not destroy the fine structure of the vorticity, which will be incorporated as fine filaments within vorticity filaments of a new spiral (figure 8).

It is worth noting the relationship between our model and Lundgren's (1982) strained spiral vortex model of three-dimensional turbulence. We may obtain one of Lundgren's three-dimensional vortices by extending our two-dimensional vorticity distribution a distance $L_0 \gg R$ into the $z$-direction (in cylindrical polar coordinates), and imposing, in addition to the process of winding up, a uniform strain $a$ along the axis of the vortex. Lundgren identifies this axial strain, due to the other vortices in the flow, by assuming that the rate of dissipation of energy in the fluid, $\mathscr{E}$, satisfies $\mathscr{E} \sim \nu a^2$. The energy spectrum of the strained vortex, $E_s(k,t)$, is related to that of the original, unstrained two-dimensional vortex by:

$$E_s(k,t) = L_0 S^{\frac{1}{2}} E(k/S^{\frac{1}{2}}, P), \tag{4.2}$$

where

$$S(t) = e^{at}, \quad P(t) = \int_0^t S(t')\,dt'. \tag{4.3}$$

Lundgren assumes that in a turbulent fluid, vortices are continually created with the same basic spiral structure, are stretched, wind up, and eventually recombine to form new short vortices. The energy spectrum of the fluid is obtained by averaging

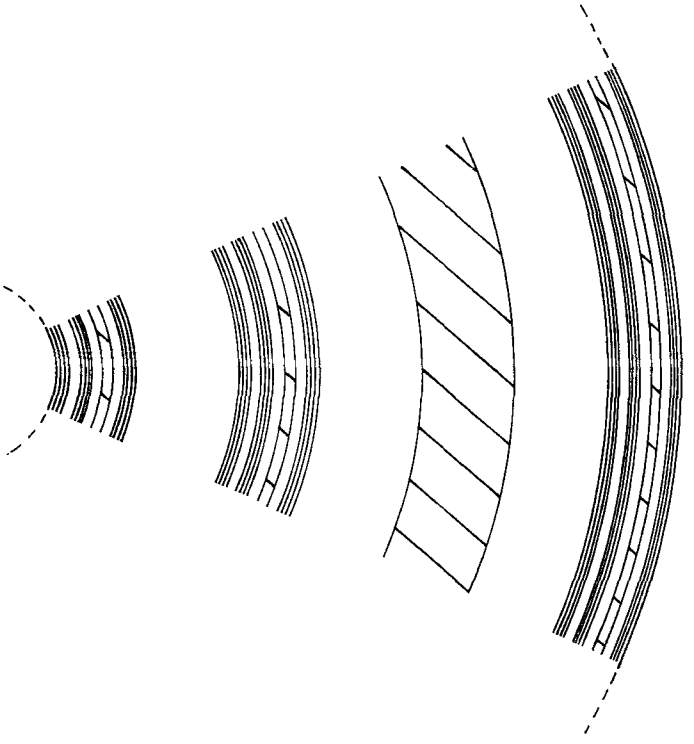

FIGURE 8. A segment of a spiral containing filaments within filaments. The vorticity is unity within the shaded regions and zero elsewhere.

the energy spectrum of a single spiral vortex over a typical lifetime and gives a range with the Kolmogorov $k^{-\frac{5}{3}}$ spectrum down to the Kolmogorov scale. The model assumes that diffusion destroys the spirals; this is reasonable in three-dimensional turbulence, because as $\nu \to 0$, $a \to \infty$ (since it is likely that $\mathscr{E}$ remains finite in this limit (Batchelor 1969)), and the spirals evolve and diffuse away faster.

### 4.1. *Fractals and self-similar spirals*

In the last section we noted that spirals are unlikely to be destroyed by diffusion in the limit of low viscosity, and instead are likely to become incorporated as fine structure within new spirals, created by vortex collisions and instabilities. This suggests that we construct a new model in which spiral filaments may themselves have a self-similar filamented structure (figure 8). Of course the details of such a self-similar spiral in the fluid will depend on the history of the vortex, its instabilities and interactions with other vortices and we shall not attempt detailed calculations of the corresponding energy spectrum. In this rather speculative section, we relate our earlier calculations to certain results on fractals, and comment on the case of self-similar spirals.

The energy spectrum of an isotropic two-dimensional flow may be related to a vorticity correlation function by

$$S(r) = \int (\omega(\boldsymbol{x}+\boldsymbol{r})-\omega(\boldsymbol{x}))^2 \,\mathrm{d}^2\boldsymbol{x} = 4\int k^2 E(k)\,(1-J_0(kr))\,\mathrm{d}k, \tag{4.4}$$

where $r = |\boldsymbol{r}|$. Now suppose the vorticity is concentrated in a vortex patch $\mathscr{D}$, whose boundary $\partial\mathscr{D}$ has a fractal dimension $d$, measured over some range of scales $r_\ell \lesssim r \lesssim r_u$. Then Ball & Kingdon (1986) have argued that

$$S(r) \sim r^{2-d} \tag{4.5}$$

in this same range of $r$. (Mandelbrot 1977 and Hentschel & Procaccia 1984 have given another relation, valid under different circumstances, as discussed in Ball & Kingdon 1986.) From (4.4), the corresponding energy spectrum for $1/r_u \lesssim k \lesssim 1/r_\ell$ is

$$E(k) \sim k^{-5+d}. \tag{4.6}$$

Since the dimension satisfies $1 \leqslant d < 2$, the spectrum is $k^{-4}$ when the boundary has no small-scale structure, in agreement with Saffman (1971), and can approach, but not attain, $k^{-3}$. This is in agreement with our earlier calculations, and an argument of Frisch (1986) that a $k^{-3}$ spectrum cannot arise from structures that are too sparse, such as fractals and spirals.

Consider now the spirals of §2, and take $\epsilon = 0$ for simplicity, so that they possess structure on indefinitely small scales. A suitable measure of the dimension of the boundary of such a spiral is its Kolmogorov capacity (see Farmer, Ott & Yorke 1983), which is easily estimated to be $d = 1 + (s-1)/(s+1)$. (The Hausdorff dimension, which is often employed, is unity here.) Our calculations of the energy spectrum confirm the relationship (4.6), and support the work of Ball & Kingdon (1986), provided that the capacity is taken as the appropriate measure of fractal dimension.

Now let us return to the problem of self-similar spirals; if the decaying turbulence is modelled by a collection of vortex patches whose boundaries have dimension $d$ over a given range of scales, then the energy spectrum of the flow will fall off as $k^{-5+d}$ in this range. Again the accumulation of approximate discontinuities in the vorticity distribution modifies the spectrum from $k^{-4}$ to a shallower spectrum. Note that the energy spectrum approaches $k^{-3}$ when the dimension of the boundary approaches two, that is, when the number of filaments at each level of the self-similar structure (figure 8) is large. Physically this is when collisions are infrequent, since each collision corresponds to a level of the self-similar structure, and the number of spiral coils at each level increases with the time between collisions. In decaying two-dimensional turbulence, coherent vortices tend to combine, so the number of vortices in the flow decreases with time, and collisions become more and more infrequent. This suggests that the energy spectrum of the flow may tend to $k^{-3}$ in the limit of long times (before very long times when the viscosity has destroyed most of the vorticity, and the flow is dominated by viscous decay). However this behaviour has not been seen in numerical simulations (B. Legras, personal communication) and so these ideas remain somewhat speculative.

## 5. Conclusions and discussion

We have shown that a spiral, formed by the passive advection of a weak vortex patch by a strong vortex, has an energy spectrum which falls off as $k^{-\frac{11}{3}}$ in the spiral range. Generalizing the velocity field, to perhaps include some average effect of the vorticity in the spiral, gives an energy spectrum with a power law lying between $k^{-3}$ and $k^{-4}$ in the spiral range. We must sum the energy spectra of all the vortices and spirals in a decaying two-dimensional flow to obtain its energy spectrum. Now suppose all the spirals are created with approximately the same structure

simultaneously, for example, when the vortices first emerge in the flow. Then the energy spectrum of the fluid will also have a fall-off of between $k^{-3}$ and $k^{-4}$ in a time-dependent spiral range. At later times there will be a continual creation of spirals by vortex collisions and instabilities. In this case it is necessary to average the instantaneous energy spectrum of a typical spiral over its lifetime, to find the energy spectrum of the flow. In Lundgren's (1982) strained spiral model of quasi-equilibrium three-dimensional turbulence, the axial stretching of the vortices accelerates the winding-up process, and the time average gives the Kolmogorov $k^{-\frac{5}{3}}$ energy spectrum. In a two-dimensional flow, the corresponding time average gives a $k^{-2}$ spectrum, at odds with theory and numerical results. However this assumes that the spirals are destroyed by diffusion, which is unlikely in two-dimensional turbulence in the limit of low viscosity. In practice, a spiral will be disrupted by interactions with other vortices, long before it diffuses away, and will acquire a self-similar 'filaments within filaments' structure. Some results on fractals (which have support from our calculations) suggest that for such a self-similar spiral the instantaneous energy spectrum also has a fall-off lying between $k^{-3}$ and $k^{-4}$, the slope being related to the fractal dimension of the boundary of the spiral.

In conclusion, our models indicate that the accumulation of approximate discontinuities in vorticity gives an instantaneous energy spectrum shallower than Saffman's (1971) $k^{-4}$ spectrum, but steeper than the $k^{-3}$ suggested by models of an enstrophy cascade. However the models are essentially kinematic; the problem remains of constructing a dynamical picture of two-dimensional turbulence that would incorporate the distribution and time evolution of characteristic structures, such as self-similar spirals, in the flow field.

In our analysis we have assumed that the vorticity is passively advected by the flow of a strong vortex (except for the minor generalization of $s \neq 2$); this suggests that our calculations might be more realistic for the advection of a truly passive scalar in a turbulent two-dimensional flow. However a passive scalar has no dynamical effects, and no tendency to form vortices. Although a patch of passive scalar close to a vortex will form a spiral, the vortices may only cover a small area of the fluid and in between the vortices the scalar will be stretched by the vortex motion. It is not clear which of these two processes is more important in the cascade of the scalar to small scales (see Babiano *et al.* 1987). In defence of our treatment of vorticity as passively advected by vortices, we may make several points. A filament of vorticity in the fluid between the vortices will be unstable and will tend to roll up and form vortices, if the flow field due to the vortices does not stretch it sufficiently quickly to suppress this instability. However a filament of a spiral will be stable provided that the shear (or differential rotation) of the nearby vortex core is sufficiently strong (T. G. Shepherd, D. G. Dritschel, personal communications); this is a consequence of Fjørtoft's (1950) stability theorem (see also Arnol'd 1965). Thus we may be justified in considering coherent vortices passively advecting filaments of vorticity, whereas the important processes for the advection of a truly passive scalar are less clear.

It is interesting to compare this picture with the results of Aref (1984) for 'stirring by chaotic advection', Aref considers passive advection by a time-periodic, two-dimensional flow in a disk driven by two point vortices which are switched on and off. An analytical integration of the motion of an advected particle over one period of the flow gives a 'return map', which, in general, possesses fixed points. Over many periods of the flow, a patch of scalar becomes distended into 'whorls' about the elliptic fixed points, and 'tendrils' about the hyperbolic fixed points.

In our picture of a two-dimensional turbulent flow, a passive scalar is stirred by the motion of coherent, extended vortices. This motion is aperiodic in general, and cannot be represented by iterations of a single return map; so the whorl and tendril structures associated with the fixed points of such maps do not occur. Although at any instant there are, in general, stagnation points of the flow, these wander at random (on the timescales of the vortex motion), and are not associated with particular blobs of fluid. In turbulent two-dimensional flows, the closest thing to a whorl is a spiral associated with a vortex; however there is no obvious analogue to a tendril.

Thus there are important differences between stirring by a turbulent two-dimensional flow, and stirring by the periodic flows considered by Aref (1984), which, although non-turbulent (in the Eulerian sense), may stir a scalar more efficiently. The singular velocity field generated by point vortices may mix a scalar better than the non-singular velocity field of an extended vortex. Also switching *fixed* point vortices on and off gives very effective stirring; when a vortex has stirred up a nearby patch of scalar, and is switched off, the flow advects the stirred scalar away, replacing it by another patch of scalar, to be stirred when the vortex is next switched on. However an extended vortex in a turbulent flow moves with the fluid and stirs up the same patch of scalar, until it is disrupted by a collision, or close encounter with another vortex.

I would like to thank H. K. Moffatt, for suggesting that I investigate this subject, for helpful discussions, and for reading earlier drafts of this paper. I would also like to thank K. Bajer, D. G. Dritschel, U. Frisch, B. Legras, P. C. Matthews, M. E. McIntyre, A. Pouquet, A. Purnama, T. G. Shepherd, J. C. Vassilicos and the referees for advice and comments. I am grateful for financial support from an SERC studentship.

## REFERENCES

Aref, H. 1984 Stirring by chaotic advection. *J. Fluid Mech.* **143**, 1.

Arnol'd, V. I. 1965 Conditions for nonlinear stability of stationary plane curvilinear flows of an ideal fluid. *Dokl. Akad. Nauk. SSSR* **162**, 975. (English transl. *Soviet Math.* **6**, 773 (1965).)

Babiano, A., Basdevant, C., Legras, B. & Sadourny, R. 1987 Vorticity and passive-scalar dynamics in two-dimensional turbulence. *J. Fluid Mech.* **183**, 379.

Ball, R. C. & Kingdon, R. D. 1986 The fractal dimension of clouds. Preprint, Cavendish Laboratory, Cambridge University.

Batchelor, G. K. 1969 Computation of the energy spectrum in homogeneous two-dimensional turbulence. *Phys. Fluids Suppl.* II, 233.

Benzi, R., Patarnello, S. & Santangelo, P. 1987 On the statistical properties of two-dimensional decaying turbulence. *Europhys. Lett.* **3**, 811.

Brachet, M. E., Meneguzzi, M. & Sulem, P. L. 1986 Small scale dynamics of high Reynolds number two-dimensional turbulence. *Phys. Rev. Lett.* **57**, 683.

Dritschel, D. G. 1988 Contour surgery: a topological reconnection scheme for extended integrations using contour dynamics. *J. Comp. Phys.* (in press).

Farmer, J. D., Ott, E. & Yorke, J. A. 1983 The dimension of chaotic attractors. *Physica* **7D**, 153.

Fjørtoft, R. 1950 Application of integral theorems in deriving criteria of stability for laminar flows and for the baroclinic circular vortex. *Geofys. Publ. Oslo* **17**, 1.

Frisch, U. 1986 Turbulence incompressible bi-dimensionnelle. *Observatoire de Nice Rep.* 82/522.

Hentschel, H. G. E. & Procaccia, I. 1984 Relative diffusion in turbulent media: the fractal dimension of clouds. *Phys. Rev.* **A29**, 1461.

HERRING, J. R. & MCWILLIAMS, J. C. 1985 Comparison of direct numerical simulation of two-dimensional turbulence with two-point closure; the effects of intermittency. *J. Fluid Mech.* **153**, 229.

HERRING, J. R., ORSZAG, S. A., KRAICHNAN, R. H. & FOX, D. G. 1974 Decay of two-dimensional homogeneous turbulence. *J. Fluid Mech.* **66**, 417.

KIDA, S. 1985 Numerical simulation of two-dimensional turbulence with high-symmetry. *J. Phys. Soc. Japan* **54**, 2840.

KRAICHNAN, R. H. & MONTGOMERY, D. 1980 Two-dimensional turbulence. *Rep. Prog. Phys.* **43**, 547.

LEGRAS, B., SANTANGELO, P. & BENZI, R. 1988 High resolution numerical experiments for forced two-dimensional turbulence. *Europhys. Lett.* **5**, 37.

LESIEUR, M., STAQUET, C., LE ROY, P. & COMTE, P. 1988 The mixing layer and its coherence examined from the point of view of two-dimensional turbulence. *J. Fluid Mech.* **192**, 511.

LUNDGREN, T. S. 1982 Strained spiral vortex model for turbulent fine structure. *Phys. Fluids* **25**, 2193.

MCWILLIAMS, J. C. 1984 The emergence of isolated coherent vortices in turbulent flow. *J. Fluid Mech.* **146**, 21.

MANDELBROT, B. B. 1977 *Fractals, Form, Chance and Dimension.* San Francisco: Freeman.

MELANDER, M. V., ZABUSKY, N. J. & MCWILLIAMS, J. C. 1987 Asymmetric vortex merger in two dimensions: which vortex is 'victorious'? *Phys. Fluids* **30**, 2610.

MOFFATT, H. K. 1984 Simple topological aspects of turbulent vorticity dynamics. In *Proc. IUTAM Symp. on Turbulence and Chaotic Phenomena in Fluids* (ed. T. Tatsumi), p. 223. Elsevier.

MOFFATT, H. K. & KAMKAR, H. 1983 The time-scale associated with flux expulsion. In *Stellar and Planetary Magnetism* (ed. A. M. Soward), p. 91. Gordon and Breach.

RHINES, P. B. & YOUNG, W. R. 1983 How rapidly is a passive scalar mixed within closed streamlines? *J. Fluid Mech.* **133**, 133.

SAFFMAN, P. G. 1971 On the spectrum and decay of random two-dimensional vorticity distributions at large Reynolds number. *Stud. Appl. Maths* **50**, 377.

WEISS, N. O. 1966 The expulsion of magnetic flux by eddies. *Proc. R. Soc. Lond.* A**293**, 310.